Journal of Applied Chemistry and Environment Protection

Corrosion Inhibition and Adsorption Behaviour of from *Foeniculum vulgare* seeds hydracid Extract on C38 Steel Corrosion in 1M HCl media

Mohamed Znini

[1] Laboratoire des Substances Naturelles & Synthèse et Dynamique Moléculaire, Faculté des Sciences et Techniques, Université My Ismail, Errachidia BP 509, 52003, Morocco.

Abstract : The inhibitive action of *Foeniculum vulgare* seeds (FVS) hydracid extract on C38 steel corrosion in 1M HCl solution was investigated by gravimetric and Tafel polarization curves techniques. The results show FVS to be a good inhibitor in acid solution. Inhibition efficiency (*IE*) increased with concentration and decreased with temperature for FV extract in HCl solution. The polarization curve of Tafel revealed that the FVS hydracid extract acts as a mixed-type inhibitor. The mechanism of adsorption proposed for FVS hydracid extract is physisorption in HCl solution and the adsorption obeys Langmuir isotherm.

Keywords: *Foeniculum vulgare*; Seeds; Hydracid extract; C38 steel; Corrosion.

1. Introduction

Corrosion, from the Latin “corrodere”, means “to chew away” or “to attack” a material as a result of chemical or electrochemical interaction between this material and its environment [1]. The consequences are significant in various fields and in particular in industry. Steel, material frequently used in industry, is corroded in specific environments and some aggressive media (acidic medium for example). Steel corrosion can be and often is the primary cause of damage to various types of infrastructure [2].

It is estimated that a one quarter of the world's annual steel production is destroyed by corrosion which represents approximately 150 million tons/year or 5 tons/sec [3]. Also, in most industrialized countries, the total cost of corrosion is estimated at between 2 and 4% of the Gross National Product (GNP) [4].

* Corresponding author. Tel.: +212 0661422903; fax: +212 0535574485. E-mail address: m.znini@yahoo.fr

In terms of protection, corrosion inhibitors are an integral means of protection against metallic corrosion. Corrosion inhibitors have the originality of being the only means of intervention from the corrosive environment, making it an easy to implement corrosion control method and inexpensive, provided that the product or products used are of moderate cost [5]. In acidic medium, the main corrosion inhibitors used are synthetic organic corrosion inhibitors; however, these compounds have the disadvantage of being toxic and polluting the environment, which has led to research other corrosion inhibitors more respectful of the environment and public health. Recently, the use of plant extracts, such as eco-friendly corrosion inhibitors, is a theme of research in development. The inhibitive action of plant extracts has been attributed to the presence of many families of natural organic compounds which are biodegradable, ecological, easily available and renewable. These phytochemical constituents (terpenoids, flavonoids, alkaloids…) act first by adsorption on the surface of the metals through active centers (N, O, S) capable of exchanging electrons with the metal [6-8]. In addition, the availability of a π electron system present in triple or conjugated double bonds or aromatic rings in the molecular structures of these compounds play a vital role in their adsorption and formation of co-ordinate bond with the metal surface [9].

Foeniculum vulgare, universally known as Fennel, is a medicinal plant belonging to the Umbelliferae (Apiaceae) family. It is a traditional and popular herb with a long history of use as a medicine. A series of studies showed that *F. vulgare* effectively controls numerous infectious disorders of bacterial, fungal, viral, mycobacterium, and protozoal origin [10,11]. Some of the publications stated that *F. vulgare* has antioxidant, antitumor, chemopreventive, cytoprotective, hepatoprotective, hypoglycemic, and oestrogenic activities [12,13].

The use of essential oils extracted from *F. vulgare* has been applied as green corrosion inhibitors for the corrosion of steel and its alloy in 1M HCl solutions [14-18]. In view of our continued interest on the application of plant extracts for steel corrosion control, we report here in investigation into the adsorption and corrosion inhibitive behaviour of acid extract of *F. vulgare* seeds (FVS) on C38 steel in HCl solutions using weight loss and Tafel polarisation methods. The influence of temperature on the adsorption behaviour of the hydracid extract on C38 steel surface and the mechanism of adsorption is discussed.

2. Experimental

2.1. Materials

Carbon steel samples (0.21% C, 0.38% Si, 0.09% P, 0.01% Al, 0.05% Mn, 0.05% S) were used. Analytical grade 37% w HCl was used for the preparation of 1 M HCl by dilution with double distilled water.

2.2. Acid extraction and preparation of inhibitor solutions

Foeniculum vulgare seeds (FVS) were obtained from a local market in Errachidia, Morocco. The seeds were cleaned and ground into powder. 4.0 g of the powder was digested for 24 h in separate 1 litre solution of 1 M HCl solution. After 24 h, the solution was filtered and the resulting solution stored as the stock solution (4.0 g/L). The stock solutions (hydracid extract) of the plant extract were used to prepare different concentrations of inhibitor (FVS) solutions ranging from (0.5 - 4.0 g/L) [19]

2.3. Weight loss measurements

2.3.1. Effect of concentration

Weight loss tests were carried out in a double walled glass cell equipped with a thermostat-cooling condenser. The solution volume was 100 mL with and without the presence of different concentrations of FVS hydracid extract ranging from 0.5 to 4 g/L at 298. After 6 h of immersion, the specimens of steel were carefully washed in double-distilled water, dried and then weighed. The rinse removed loose segments of the film of the corroded samples. Triplicate experiments were performed in each case and the mean value of the weight loss is reported using an analytical balance (precision ± 0.1 mg). Weight loss allowed us to calculate the mean corrosion rate as expressed in $mg.cm^{-2}\ h^{-1}$.

The corrosion rate (W_{corr}) and inhibition efficiency Ew (%) were calculated according to the Eqs. (1) and (2) respectively:

$$W = \frac{\Delta m}{St} \qquad (1)$$

$$E_W\ \% = \frac{W_{corr} - W_{corr\,(inh)}}{W_{corr}} \times 100 \qquad (2)$$

where Δm (mg) is the specimen weight before and after immersion in the tested solution, W_{corr} and $W_{corr(inh)}$ are the values of corrosion weight losses ($mg/cm^2.h$) of mild steel in uninhibited and inhibited solutions, respectively, S is the area of the mild steel specimen (cm^2) and t is the exposure time (h).

2.3.1. Effect of temperature

The effect of temperature on the inhibited acid–metal reaction is very complex, because many changes occur on the metal surface such as rapid etching, desorption of inhibitor and the inhibitor itself may undergo decomposition. The change of the corrosion rate with the temperature was studied in 1 M HCl during 1 h of immersion, both in the absence and presence of inhibitor at a concentration corresponding to the maximum inhibition efficiency. For this purpose, gravimetric experiments were performed at different temperatures

(298–338 K). To calculate activation thermodynamic parameters of the corrosion process, Arrhenius Eq. (3) and transition state Eq. (4) were used [6]:

$$W = A\exp(-\frac{E^{\circ}_{a}}{RT}) \quad (3)$$

$$W = \frac{RT}{Nh}\exp(\frac{\Delta S^{\circ}_{a}}{R})\exp(-\frac{\Delta H^{\circ}_{a}}{RT}) \quad (4)$$

where E°a is the apparent activation corrosion energy, R is the universal gas constant, A is the Arrhenius preexponential factor, h is the Plank's constant, N is the Avogrado's number, ΔS°a is the entropy of activation and ΔH°a is the enthalpy of activation.

2.4. Potentiodynamic polarization curves

The measurements were carried out in a conventional three-electrode electrolysis cylindrical Pyrex glass cell. The working electrode (WE) in the form of disc cut from steel has a geometric area of 1 cm2 and is embedded in polytetrafluoroethylene (PTFE). A saturated calomel electrode (SCE) and a disc platinum electrode were used respectively as reference and auxiliary electrodes, respectively. The temperature was thermostatically controlled at 298 K. The WE was abraded with silicon carbide paper (grade P1200), degreased with AR grade ethanol and acetone, and rinsed with double distilled water before use.

Polarization curves studies were carried out using Amel potentiostat-galvanosta (model 549) at 298 K without and with addition of various concentrations of FVS hydracid extract (0.5-4 g/L) in 1 M HCl solution at a scan rate of 0.5 mV/sec. Before recording the cathodic polarisation curves, the mild steel electrode is polarised at -700 mV for 10 min. For anodic curves, the potential of the electrode is swept from its corrosion potential after 20 min at free corrosion potential, to more positive values. The test solution is deaerated with pure nitrogen. Gas bubbling is maintained through the experiments.

In the case of polarization method the relation determines the inhibition efficiency (E_I %):

$$E_I\% = \frac{I_{corr} - I_{corr(inh)}}{I_{corr}} \times 100 \quad (5)$$

where I_{corr} and $I_{corr\ (inh)}$ are the corrosion current density values without and with the inhibitor, respectively, obtained by extrapolation of cathodic and anodic Tafel lines to the corrosion potential.

2.5. Adsorption isotherm and thermodynamics parameters

The mechanism of the interaction between inhibitor and the metal surface can be explained using adsorption isotherms. In order to obtain the adsorption isotherm, the degree of surface coverage (θ) of the inhibitors must be calculated with several adsorption isotherms, including Langmuir, Frumkin, and Temkin. In this study, the degree of surface coverage values (θ) for various concentrations of the inhibitor in acidic media have been evaluated from the Weight loss measurements

3. Results and discussion

3.1. Weight loss measurements

3.1.1. Effect of concentration

The values of percentage inhibition efficiency Ew (%) and corrosion rate (W) obtained at different concentrations of FVS hydracid extract at 298 K are summarized in Table 1 and Fig. 1.

Table 1. Weight loss results of C38 steel in 1 M HCl without and with different concentrations of FVS hydracid extract (t= 6h, T= 298 K)

Concentration (g/L)	W (mg/h.cm2)	Ew (%)
0	0.381	--
0.5	0.045	88
1	0.037	90
1.5	0.033	91
2	0.031	92
4	0.023	94

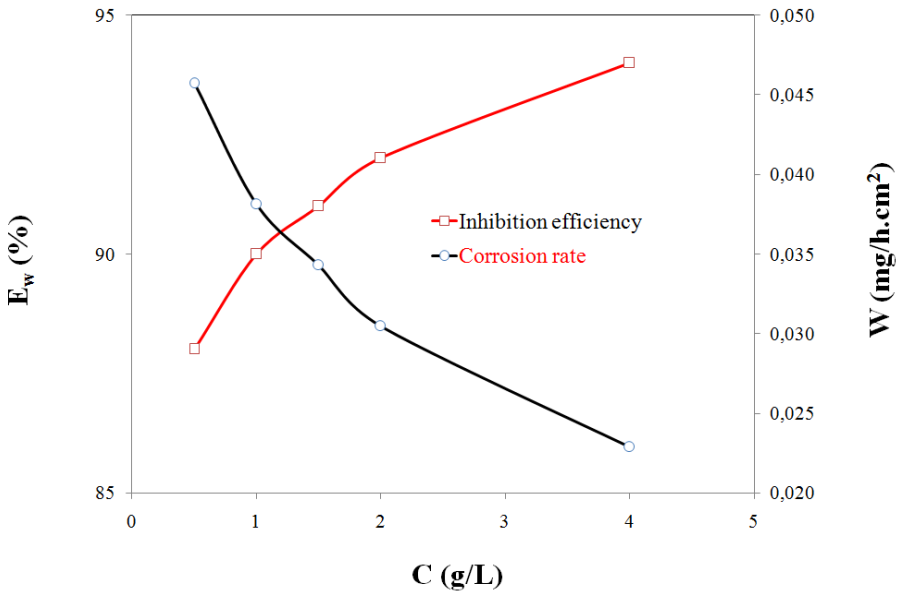

Fig. 1. Variation of corrosion rate (W) and inhibition efficiency (Ew) of corrosion of C38 steel in 1 M HCl with different concentration FVS hydracid extract

The results obtained in Table 1 and Fig. 1 indicated that the corrosion rate (W) of C38 steel decreased continuously with increasing the inhibitor concentration, ie, the corrosion of steel is retarded by FVS hydracid extract. However, the inhibition efficiency Ew increases sharply with increase in concentration of inhibitor reaching a maximum value of 94 % at 4 g/L. This behavior could be explained by the adsorption of phytochemical components of the FVS hydracid extract onto the C38 steel surface resulting in the blocking of the reaction sites, and protection of the C38 steel surface from the attack of the corrosion active ions in the acid medium [20]. Consequently, we can conclude that the FVS hydracid extract is a good corrosion inhibitor for mild steel in 1 M HCl solution.

3.1.2. Effect of temperature

The effect of temperature on the corrosion behaviour of C38 steel in 1 M HCl containing FVS hydracid extract at 4 g/L is studied in the temperature range 298-338 K using weight loss measurements at 1 h. The data of corrosion rates (W) and corresponding efficiency (Ew) collected were presented in Table 2 and Fig 2.

Table 2. Corrosion parameters obtained from weight loss for C38 steel in 1 M HCl containing 4 g/L of FVS hydracid extract at different temperatures

T (K)	W_{inh} mg/cm^2.h	W_0 mg/cm^2.h	Ew %
298	0.209	4.178	95
303	0.668	7.419	91
318	1.230	11.178	89
328	2.084	17.369	88
338	2.712	19.369	86

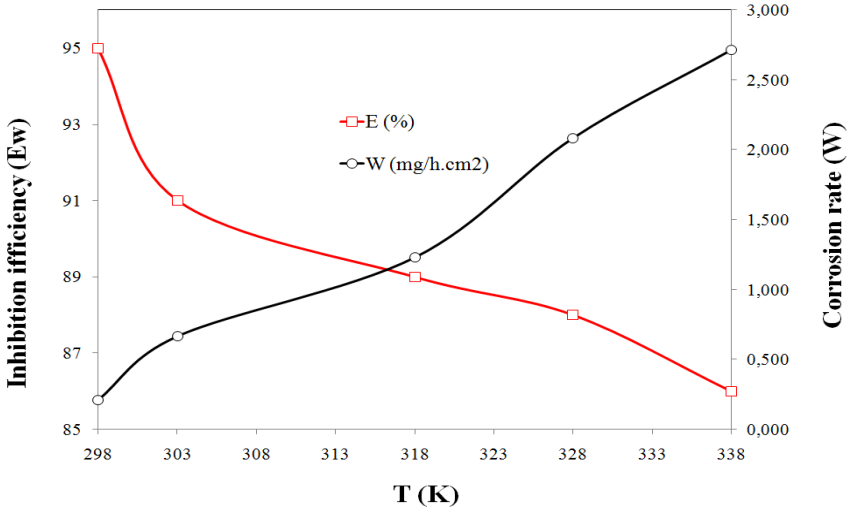

Fig. 2: Variation of corrosion rate (W) and inhibition efficiency (Ew) of corrosion of C38 steel in 1 M HCl with different temperatures in the presence of 4 g/L of FVS hydracid extract

Inspection of these results reveals that the corrosion rate (W) increases with temperature both in uninhibited and inhibited solutions especially goes up more rapidly in the absence of inhibitor. This result indicates that the presence of inhibitor leads to decrease of the corrosion rate. Also, we note that the efficiency (Ew) depends on the temperature and decreases with the rise of temperature from 298 to 338 K. These behaviour may be attributed to the increased desorption of inhibitor molecules from metal surface and the increase in the solubility of the protective film or the reaction products precipitated on the surface of the metal that might otherwise inhibit the reaction [21].

3.2. Activation parameters $E°_a$, $\Delta S°_a$, $\Delta H°_a$

In order to calculate activation parameters of the corrosion reaction such as activation energy $E°_a$, activated entropy $\Delta S°_a$ and enthalpy $\Delta H°_a$, the Arrhenius equation (Eq. (3)) and its alternative formulation called transition state equation (Eq. (4)) were employed. Plotting the logarithm of the corrosion rate (W) versus reciprocal of absolute temperature (1/T), the activation energy can be calculated from the slope (-E°a/R). Fig. 3 shows the variations of Ln W with the presence and absence of inhibitor with the (10^3/T).

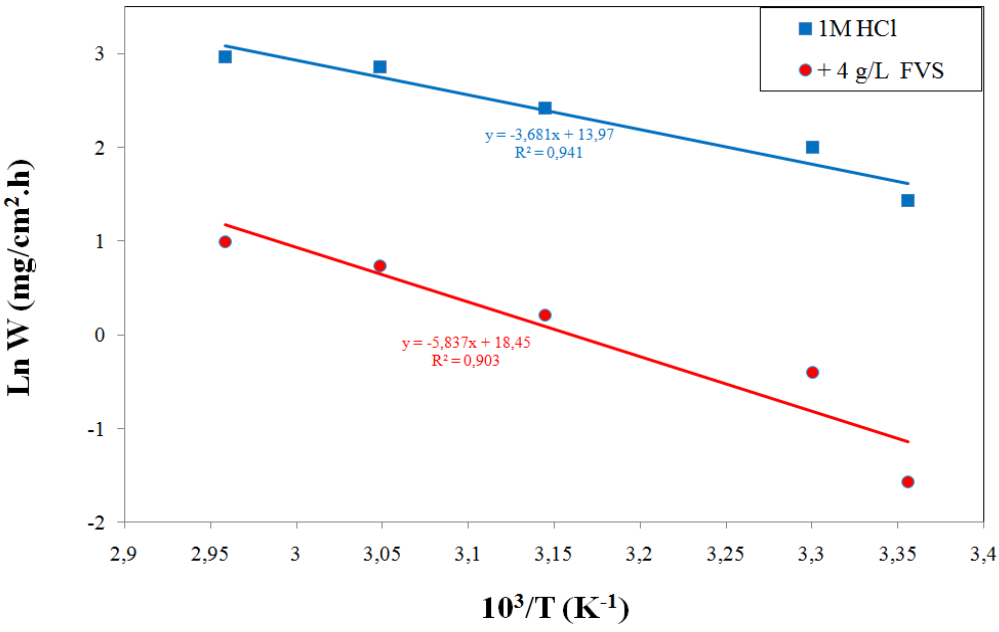

Fig. 3. Arrhenius plots for C38 steel corrosion rates (W) in 1 M HCl in absence and in presence of 4 g/L of FVS hydracid extract

The logarithm of the corrosion rate of steel (Ln W) can be represented as straight-lines function of (10^3/T) with the linear regression coefficient (R^2) was close to 1, indicating that the corrosion of steel in hydrochloric acid without and with inhibitor follows the Arrhenius equation. The activation energy ($E°_a$) values were calculated from the Arrhenius plots (Fig. 3) and the results are shown in Table 3.

Further, using Eq. (4), plots of Ln (W/T) versus 10^3/T gave straight lines (Fig. 4) with a slope of ($-\Delta H°_a/R$) and an intercept of ($Ln(R/Nh) + (\Delta S°_a/R)$) from which the values of $\Delta H°_a$ and $\Delta S°_a$ were calculated and are listed in Table 3.

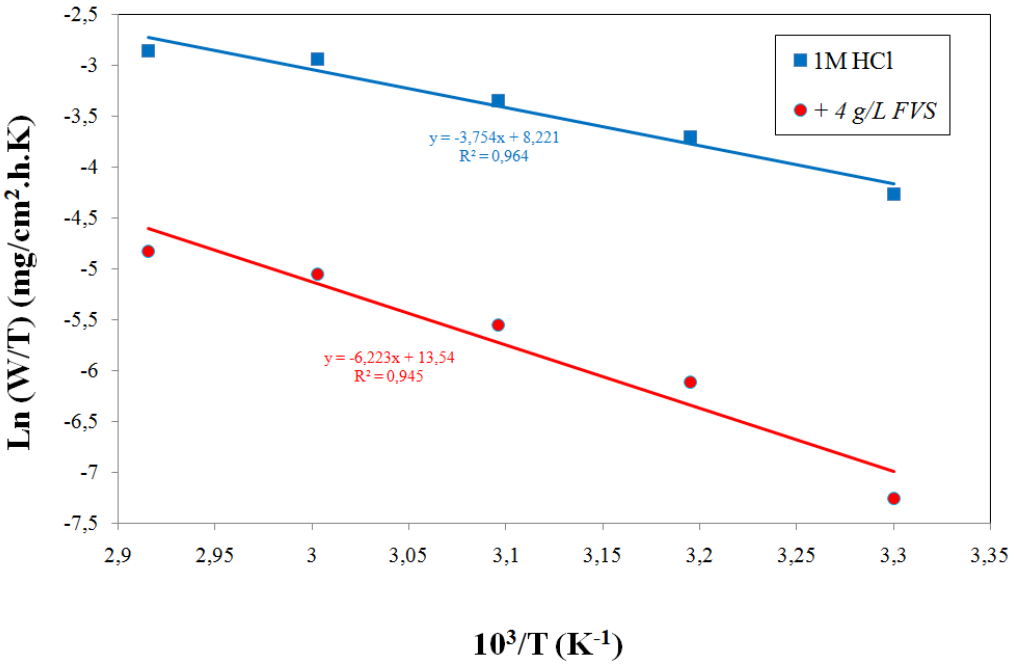

Fig. 4. Transition-state plots for C38 steel corrosion rates (W) in 1 M HCl in absence and in presence of 4 g/L of FVS hydracid extract

Table 3. Activation parameters $E°_a$, $\Delta S_a°$, $\Delta H°_a$ of the dissolution of C38 steel in 1 M HCl in the absence and presence of 4 g/L of FVS hydracid extract

	$E°_a$ (KJ. mol^{-1})	$\Delta H°_a$ (KJ.mol^{-1})	$\Delta S°_a$ (J. $mol^{-1}.K^{-1}$)
1M HCl	30.63	31.23	-129
+4 g/L of FVS hydracid extract	48.56	51.78	-75.18

The calculated values of activation energies from the slopes are 30.63 and 48.56 KJ.mol^{-1} for free acid and with the addition of 4 g/L of FVS hydracid extract, respectively. We remark that the activation energy increases in the presence of inhibitor. Generally, the higher E°a value leads to the lower corrosion rate and indicate that a strong inhibitive action of the additives by increasing energy barrier for the corrosion process, emphasizing the electrostatic character of the inhibitor's adsorption on the mild steel surface [22]. In addition, the value of E°a that is around 40–80 KJ.mol^{-1} can be suggested to obey the physical adsorption (physiosorption) mechanism [23].

Moreover, inspection of the data of Table 3 reveals that the positive signs of ΔH°a both in the absence and presence of 4 g/L of FVS hydracid extract reflect the endothermic nature of the mild steel dissolution process suggesting that the dissolution of mild steel is slow [24]. Typically, enthalpy of physical adsorption process is lower than 80 KJ.mol^{-1} while the enthalpy of chemisorption process approaches 100 KJ.mol^{-1} [25]. The value of the obtained enthalpy, therefore, suggests physical adsorption of the components of the FVS hydracid extract on the surface of the metal. Contrariwise, the negative values of entropies of activation (ΔS°a) imply that the activated complex in the rate determining step represents an association rather than a dissociation step, meaning that a decrease in disordering takes place on going from reactants to the activated complex [26].

3.3. Potentiodynamic polarization curves

Current-potential characteristics resulting from cathodic polarisation curves of C38 steel in 1 M HCl at various concentrations of FVS hydracid extract is evaluated. Fig. 5 (a) shows the typical cathodic Tafel plots of the tested extract at different concentrations. Table 4 collects the corrosion kinetic parameters such as Ecorr, Icorr and βc obtained from potentiodynamic polarization curves for C38 steel in 1M HCl containing different concentrations of FVS hydracid extract.

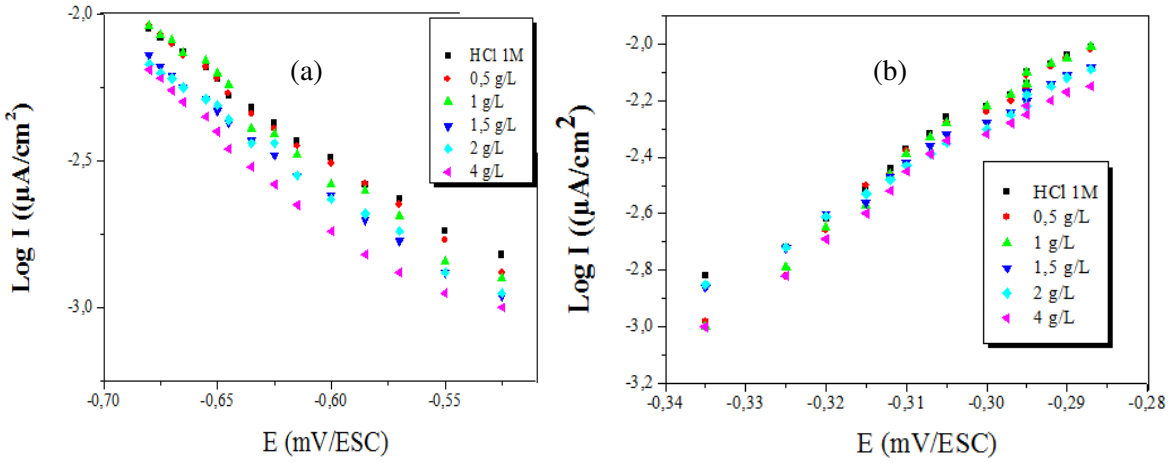

Fig. 5. Cathodic (a) and anodic curves of C38 steel in 1M HCl at various concentrations of FVS hydracid extract

Table 4. Electrochemical parameters of steel at various concentrations of FVS hydracid extract studied in 1M HCl at 298 K. Corresponding corrosion inhibition efficiencies

C (g/L)	E_{corr} (mV /cm)	i_0 (µA/cm^2)	β_a (mV/dec)	β_c (mV/dec)	E_I (%)
0	-385	450	0.014	-0.004	-
0.5	-365	135	0.02	-0.005	70
1	-380	117	0.018	-0.0047	74
1.5	-395	63	0.013	-0.0047	86
2	-400	49.5	0.011	-0.0053	89
4	-375	31.5	0,018	-0,0054	93

From Table 4, it is clear from the results that the addition of inhibitor causes a decrease of the current density. The values I_{corr} of steel in the inhibited solution are smaller than those for the inhibitor free solution. The parallel cathodic Tafel plots obtained in Figure 5 indicate that the hydrogen evolution is activation-controlled and the reduction mechanism is not affected by the presence of inhibitor. The addition of inhibitor does not change the values of cathodic Tafel slope (βc) when the concentration increases. These results demonstrate that the hydrogen evolution reaction is inhibited and that the inhibition efficiency increases with inhibitor concentration. In the anodic range (Fig. 5 (b)), the polarisation curves of steel show that the addition of the hydracids extract decreases the current densities in large domain of potential. This result suggests that this compound act as a mixed-type inhibitor.

3.4. Adsorption isotherm and thermodynamics parameters

The dependence of the fraction of the surface covered Θ obtained by the ratio E%/100 as function of the oil concentration (C) was graphically fitted for Langmuir, Temkin and Frumkin adsorption isotherms. By far, the best fit was found to obey Langmuir adsorption isotherm (Fig. 6), which may be formulated as in Eq. (6)

$$\frac{C_{inh}}{\theta} = \frac{1}{K} + C_{inh} \qquad (6)$$

where K is the adsorption equilibrium constant of the inhibitor, C_{inh} is the inhibitor concentration, and Θ is the surface coverage.

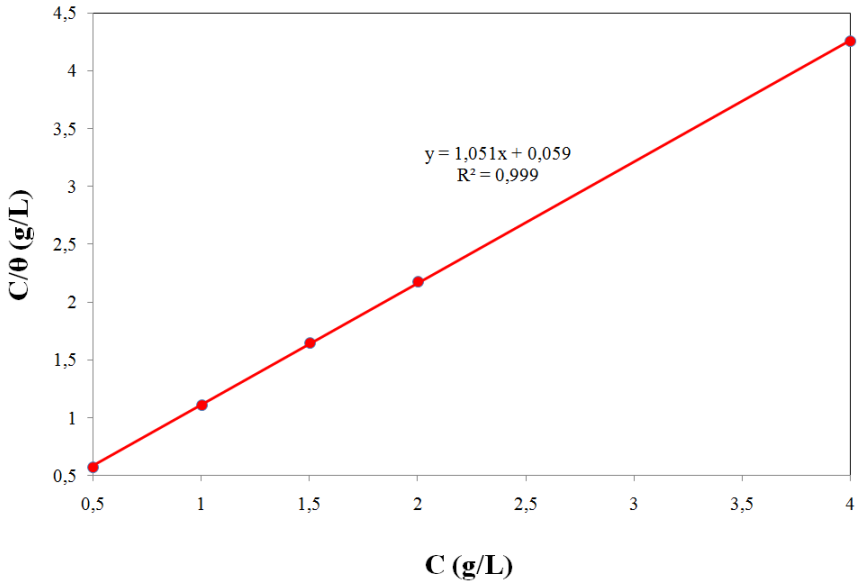

Fig. 6. Langmuir adsorption isotherm of FVS hydracid extract on the C38 steel surface in 1 M HCl at 298 K.

Thermodynamic parameters are important to further understand the adsorption process of inhibitor on steel/solution interface. The equilibrium adsorption constant, K is related to the standard Gibb's free energy of adsorption (ΔG°ads) with the following equation:

$$K = \frac{1}{55.5}.\exp\left(-\frac{\Delta G°_{ads}}{RT}\right) \quad (7)$$

where R is the universal gas constant, T is the thermodynamic temperature and the value of 55.5 is the concentration of water in the solution in mol/L (10^3 g/L).

The calculated value of free energy of adsorption was found to be ΔG°ads = −24.14 KJ.mol^{-1}, where adsorption–desorption equilibrium constant K value was obtained from the linear regression of Langmuir isotherm (K= 16.95 L/g). The negative value of ΔG°ads indicates that the inhibitor, in this case FVS hydracid extract is spontaneously adsorbed onto the mild steel surface. It is well known that values of ΔG°ads around −20 KJ.mol^{-1} or lower are associated with the physiosorption phenomenon where the electrostatic interaction assemble between the charged molecule and the charged metal, while those around −40 KJ.mol^{-1} or higher are associated with the chemiosorption phenomenon where the sharing or transfer of organic molecules charge with the metal surface occurs [27]. Hence, it is clear that FVS hydracid extract is physically adsorbed onto the C38 steel surface. Moreover, the decrease of inhibition efficiency with the increase in temperature may supports that the adsorption of FVS hydracid extract on the mild steel surface is physical in nature. As the temperature increases, the number of adsorbed molecules decreases, leading to a decrease in the inhibition efficiency.

3.5. Mechanism of corrosion inhibition

Accordingly, the effectiveness of inhibiting corrosion by plant extract could be attributed to the adsorption of its phytochemical components on the C38 steel surface. Owing to the complex chemical composition of the FVS hydracid extract, it is quite difficult to assign the inhibitive effect to a particular constituent. This makes it difficult to assign the inhibitive effect to adsorption of any particular constituent since some of these constituents including hetero-atom in functional groups (C=O, C–O, C-N, N-O, N-H, O-H….) and π-electrons of the aromatic ring or the double and triple bonds in their structure are known to exhibit inhibiting action. These organic molecules of FVS hydracid extract exist either as neutral molecules or in the form of protonated organic molecules (cation) in aqueous acidic solution.

Generally, two modes of adsorption are considered on the metal surface in acid media [28]. In first mode, if the metal surface is negatively charged with respect to potential of zero charge (PZC), the protonated amino acids would be directly adsorbed on the metal surface (Figure 7 (a)). However, if the metal surface is positively charged, it is well known that it is difficult for the protonated molecules to approach C38 steel surface (H_3O^+/metal interface) due to the electrostatic repulsion. Since Cl^- have a smaller degree of hydration, they could bring excess negative charges in the vicinity of the interface and favour more adsorption of the positively charged inhibitor molecules, the protonated inhibitors adsorb through electrostatic interactions between the positively charged molecules and the negatively charged metal surface. Thus, there is a synergism between adsorbed Cl^- ions and protonated inhibitors (Figure 7 (b)). In second mode, the neutral molecules may be adsorbed on the surface of C38 steel through the chemisorption mechanism, involving the displacement of water molecules from the metal surface and the sharing electrons between the hetroatoms and iron. The inhibitor molecules can also adsorb on the C38 steel surface on the basis of donor–acceptor interactions between their π-electrons and vacant d-orbitals of surface iron (Figure 7 (c)). In other side, the inhibiting effect of phytochemical compounds on metal corrosion was attributed to the formation of insoluble complex between the metallic ions present on surface and the phytochemical compounds via functional groups (Fig. 7(d)).

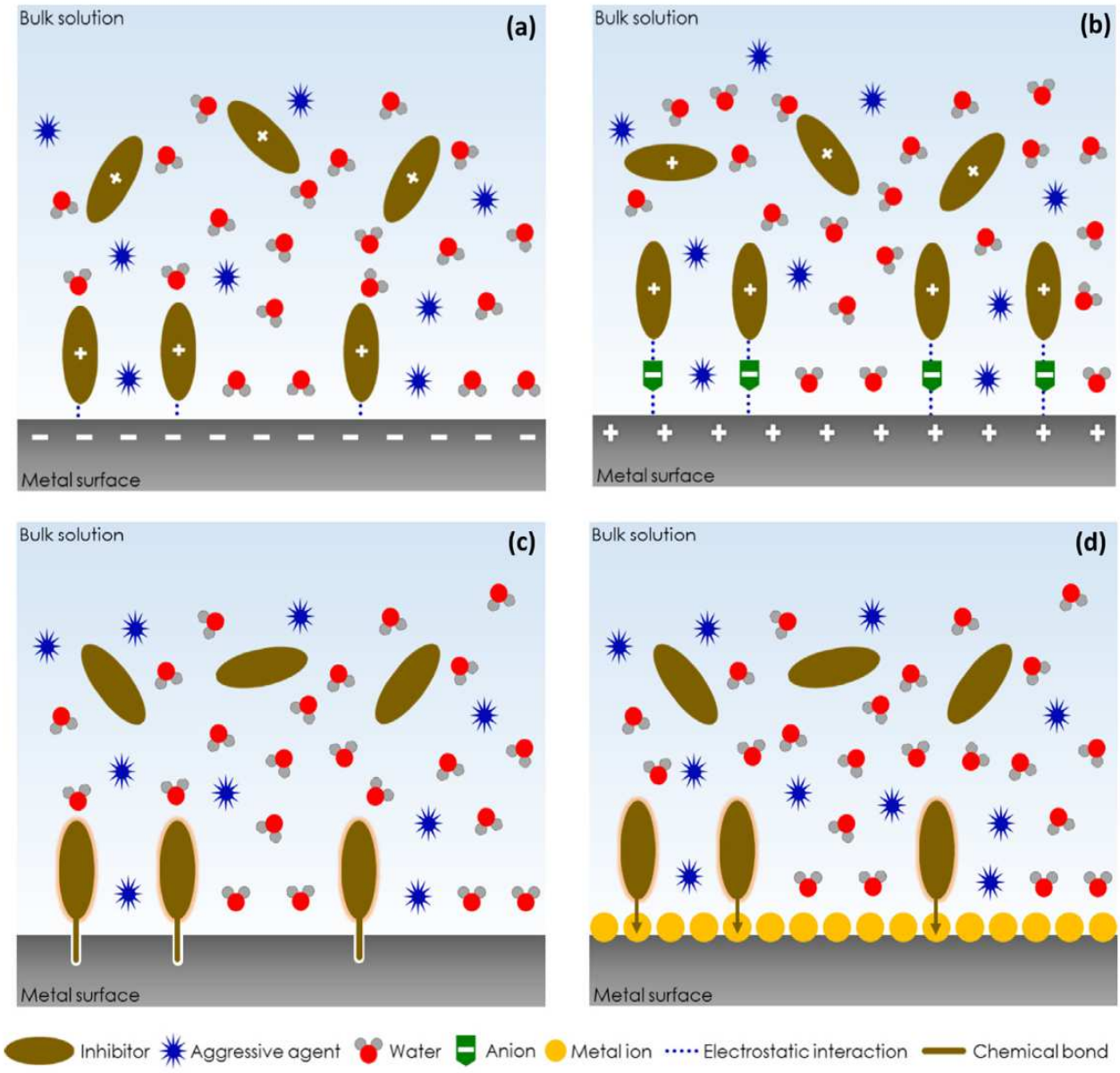

Fig. 7. Simplified schema of some interaction modes of FVS hydracid extract with metallic surface in inhibition process [28]

4. Conclusion

The inhibition action of this FVS hydracid extract can be attributed to the adsorption of its phytochemical compounds. From loss measurements, is clear that inhibition efficiency values increased with increase in inhibitor concentration but decreased with increase in temperature. The value of apparent activation energy increased with the increase in the inhibitor concentration. Enthalpy of activation reflects the endothermic nature of the mild steel dissolution process. Entropy of activation increased with increasing inhibitor concentration; hence increase in the disorderliness of the system. The adsorption behavior can be described

by the Langmuir adsorption isotherm. Gibbs free energy of adsorption indicated that the adsorption process is spontaneous and the molecules adsorbed on the metal surface by the process of physical adsorption. Results extracted by polarization curves revealed that the FVS hydracid extract acts like mixed type inhibitor.

References

1. Z. Chen, D. Koleva, K. van Breugel. Corros. Rev. 35 (2017) 397.
2. G. Blustein, J. Rodriguez, R. Romanogli, C.F. Zinola, Corro. Sci. 47 (2005) 369.
3. D. Landolt. Corrosion and surface chemistry of metals, 1st ed., Switzerland: EPFL Press, (2007).
4. J. Kruger, Cost of metallic corrosion , in Uhlig ' s Corrosion Handbook, 2nd edition , R. W. Revie , editor, Wiley , New York , (2000) 3- 10.
5. V.S. Sastri. Corrosion Inhibitors Principles and Applications. John Wiley & Sons: New York; (1998).
6. M. Znini, G. Cristofari, L. Majidi, A. Ansari, A. Bouyanzer, J. Paolini, J Costa, B. Hammouti. Int. J. Electrochem. Sci. 7 (2012) 3959.
7. M. Znini, L. Majidi, A. Bouyanzer, J. Paolini, J.-M. Desjobert, J. Costa, B. Hammouti. Arab. J. Chem. 5 (2012) 467.
8. M. Manssouri, M. Znini, A. Ansari, A. Bouyenzer, Z. Faska and L. Majidi. Der Pharma Chem. 6 (2014) 331.
9. B.M. Praveen, T.V. Venkatesha. Int. J. Electrochem. Sci. 4 (2009) 267.
10. G.J. Kaur, D.S. Arora. BMC Compl. Alter. Med. 9 (2009) 30.
11. I.E. Orhan, B. Ozcelik, M. Kartal, Y. Kan. Turk. J. Biol. 36 (2012) 239.
12. T. Malini, G. Vanithakumari, N. Megala, S. Anusya, K. Devi, V. Elango. Ind. J. Physiol. Pharmacol. 29 (1985) 21.
13. M. Oktay, I. Gulcin, O.I.K. Eufrevioglu. LWT-Food Sci. Technol. 36 (2003) 263.
14. N. Lahhit, A. Bouyanzer, J.-M. Desjobert, B. Hammouti, R. Salghi, J. Costa, C. Jama, F. Bentiss, L. Majid. Portug. Electroch. Acta. 29 (2011) 127.
15. A. Bouoidina, M.Chaouch, A. Abdellaoui, A. lahkimi, B. Hammouti, F. El-Hajjaji, M. Taleb, A. Nahle. Anti-Corros. Meth. Mat. 6 (2017) 563.
16. A. Bouoidina, F. El-Hajjaji, A. Abdellaoui, Z. Rais, M. Filali Baba M. Chaouch, O. Karzazi, A. Lahkimi, M. Taleb. J. Mater. Environ. Sci. 8 (2017) 1328.
17. A. Bouoidina, F. El-Hajjaji, M. Chaouch, A. Abdellaoui, H. Elmsellem, Z. Rais, M. Filali Baba, A. Lahkimi, B. Hammouti, M. Taleb. Der Pharma Chem. 8 (2016) 149.
18. A.S. Fouda, S.M. Rashwan, H.A. Abo-Mosallam. Desal. Water Treat. (2013) 1–12. doi: 10.1080/19443994.2013.806223.

19. M.E. Ikpi1, I.I. Udoh1, P.C. Okafor, U.J. Ekpeand E.E. Ebenso. Int. J. Electrochem. Sci. 7 (2012) 12193.
20. G. Cristofari, M. Znini, L. Majidi, A. Bouyanzer, S.S. Al-Deyab, J. Paolini, B. Hammouti, J. Costa. Int. J. Electrochem. Sci. 6 (2011) 6699.
21. M. Manssouri, Y. El Ouadi, M. Znini, J. Costa, A. Bouyanzer, J.M. Desjobert, L. Majidi, J. Mater. Environ. Sci. 6 (2015) 631.
22. M.I. Awad. J. Appl. Electrochem. 36 (2006) 1163.
23. K.O. Orubite, N.C. Oforka. Mater. Lett. 58 (2004) 1772.
24. N.M. Guan, L. Xueming, L. Fei. Mater. Chem. Phys. 86 (2004) 59.
25. S. Martinez, I. Stern. Appl. Surf. Sci. 199 (2002) 83.
26. S. Samkarapapaavinasam, M.F. Ahmed. J. Appl. Electrochem. 22 (1992) 390.
27. E. Kamis, F. Belluci, R.M. Latanision, E.S.H. El-Ashry. Corrosion 47 (1991) 677.
28. B. El Ibrahimi, A. Jmiai, L. Bazzi, S. El Issami. Arab. J. Chem. (2017). http://dx.doi.org/10.1016/j.arabjc.2017.07.013.

JACEP

ISSN: 2509-1468